



HHS Public Access

Author manuscript

Ophthalmic Surg Lasers Imaging. Author manuscript; available in PMC 2019 March 01.

Published in final edited form as:

Ophthalmic Surg Lasers Imaging. 2012 ; 43(3): 252–256. doi:10.3928/15428877-20120308-04.

Single-Shot Dimension Measurements of the Mouse Eye Using SD-OCT

Minshan Jiang, PhD[#],

Department of Ophthalmology, Optical Electronic Information and Computer Engineering College, University of Shanghai for Science and Technology, Shanghai, People's Republic of China

Pei-Chang Wu, MD, PhD[#],

Institute for Genetic Medicine, Keck School of Medicine, University of Southern California, Los Angeles, California

Department of Ophthalmology, Chang Gung Memorial Hospital-Kaohsiung Medical Center, and Chang Gung University College of Medicine, Taiwan.

M. Elizabeth Fini, PhD,

Department of Ophthalmology, Optical Electronic Information and Computer Engineering College, University of Shanghai for Science and Technology, Shanghai, People's Republic of China

Institute for Genetic Medicine, Keck School of Medicine, University of Southern California, Los Angeles, California

Chia-Ling Tsai, BDS, MS,

Department of Pediatric Dentistry, Chang Gung Memorial Hospital-Kaohsiung Medical Center, and Chang Gung University College of Medicine, Taiwan.

Tatsuo Itakura, PhD,

Institute for Genetic Medicine, Keck School of Medicine, University of Southern California, Los Angeles, California

Xiangyang Zhang, PhD, and

Department of Ophthalmology, Optical Electronic Information and Computer Engineering College, University of Shanghai for Science and Technology, Shanghai, People's Republic of China

Shuliang Jiao, PhD

Department of Ophthalmology, Optical Electronic Information and Computer Engineering College, University of Shanghai for Science and Technology, Shanghai, People's Republic of China

[#] These authors contributed equally to this work.

Abstract

The authors demonstrate the feasibility and advantage of spectral-domain optical coherence tomography (SD-OCT) for single-shot ocular biometric measurement during the development of the mouse eye. A high-resolution SD-OCT system was built for single-shot imaging of the whole

Address correspondence to Shuliang Jiao, PhD, DVRC 307, University of Southern California, 1450 San Pablo Street, Los Angeles, CA 90033. sjiao@usc.edu.

The authors have no financial or proprietary interest in the materials presented herein.

mouse eye in vivo. The axial resolution and imaging depth of the system are 4.5 μm (in tissue) and 5.2 mm, respectively. The system is capable of acquiring a cross-sectional OCT image consisting of 2,048 depth scans in 85 ms. The imaging capability of the SD-OCT system was validated by imaging the normal ocular growth and experimental myopia model using C57BL/6J mice. The biometric dimensions of the mouse eye can be calculated directly from one snapshot of the SD-OCT image. The biometric parameters of the mouse eye including axial length, corneal thickness, anterior chamber depth, lens thickness, vitreous chamber depth, and retinal thickness were successfully measured by the SD-OCT. In the normal ocular growth group, the axial length increased significantly from 28 to 82 days of age ($P < .001$). The lens thickness increased and the vitreous chamber depth decreased significantly during this period ($P < .001$ and $P = .001$, respectively). In the experimental myopia group, there were significant increases in vitreous chamber depth and axial length in comparison to the control eyes ($P = .040$ and $P < .001$, respectively). SD-OCT is capable of providing single-shot direct, fast, and high-resolution measurements of the dimensions of young and adult mouse eyes. As a result, SD-OCT is a potentially powerful tool that can be easily applied to research in eye development and myopia using small animal models.

INTRODUCTION

Due to the recent complete genomic sequence disclosure,¹ the mouse eye has become an important model for research on eye growth and myopia. To facilitate the research, there is a need for a simple, non-invasive, fast, and accurate technique to measure the structure of the mouse eye. However, there is no efficient imaging technique to fulfill this need to date. A-scan ultrasonography is a widely used technique for measuring the eye dimensions of humans and large animals.²⁻⁶ However, due to limitations in the depth of focus and resolution, it is not suitable for measuring eye dimensions in small animals such as mice. Several studies have been made to measure the dimensions of the mouse eye, including using frozen sections with or without fixation,⁷ optical low coherence interferometer,⁸ time-domain optical coherence tomography (TD-OCT),⁹ and high-resolution magnetic resonance imaging (MRI).¹⁰ The drawbacks of using postmortem eye sections are that it is difficult to simulate the status of a living eye and impossible to conduct longitudinal studies using the same animal. There might be bias caused by intraocular pressure change after enucleation and dehydration. Optical low coherence interferometer is the one-dimensional version of OCT, the same as comparing A-scan ultrasound to B-scan ultrasound. Because the optical low coherence interferometer can only obtain one-dimensional measurement, the lateral position of the measurement is unknown. The drawback of TDO-CT is its slow imaging speed. High-resolution MRI is not only time-consuming for image reconstruction but also insufficient in resolution.

Spectral-domain OCT (SD-OCT) is a relatively new extension of the OCT technology by using spectral-domain detection. Due to its advantages of much higher imaging speed and better signal-to-noise ratio, SD-OCT is becoming one of the major retinal imaging techniques not only for humans but also for small animals. In this study, we have successfully achieved single-shot measurements of the dimensions of the mouse eye by

using SD-OCT. The study demonstrated the feasibility and advantage of SD-OCT for ocular biometric measurement during development of the mouse eye.

REPORT

Animals

All experiments were performed in compliance with the Association for Research in Vision and Ophthalmology Statement for the Use of Animals in Ophthalmic and Vision Research and with the guidelines of the Institutional Animal Care and Use Committee of University of Southern California.

For the normal ocular growth group, 8 eyes of C57BL/6J mice (Jackson Laboratory) were used to assess the capability of the SD-OCT system in ocular biometric measurements. SD-OCT imaging was started when the mice were 4 weeks old.

For the experimental myopia group, hemispherical plastic diffusers were sutured to the skin surrounding the right eye with one continuous stitch at the age of 28 days. The left eye served as a control. This procedure was performed under anesthesia as described later. The animals recovered on a warming pad and were monitored until fully mobile. Treated animals were housed in transparent plastic cages under 12 hours light and 12 hours dark conditions for 21 days.

Animals were anesthetized 10 minutes before the imaging experiments by intraperitoneal injection of a cocktail containing ketamine (90 mg/kg body weight) and xylazine (10 mg/kg body weight). In the mean-time, the pupils were dilated with 1% tropicamide solution. Drops of saline solution were applied to the eyes to prevent corneal dehydration.

Imaging System and Study Procedure

The configuration of the OCT system was similar to that reported before⁹ except for some specific parameters. A superluminescent diode laser (bandwidth = 50 nm, central wavelength = 840 nm; Superlum, Moscow, Russia) was used as the light source. The low-coherence light was coupled into the source arm of a fiber-based Michelson interferometer that consists of a 2×2 3dB fiber coupler, which split the source light into the sample and the reference arms. The sample arm was interfaced to a slit lamp, which consisted of an X-Y galvanometer scanner and the optics for delivering the probing light to the mouse eye and collecting the back-reflected probing light. The power of the light at the surface of the cornea was 0.8 mW. In the detection arm, a spectrometer consisting of a 1,800 line/mm transmission grating, an achromatic imaging lens ($f = 150$ mm), and a line scan charge coupled device camera was used to detect the combined reference and sample light. The imaging depth range was 5.2 mm in air. An image acquisition board acquired the image captured by the camera and transferred it to a computer workstation for signal processing and image display. A cross-sectional OCT image consisting of 2,048 A-scans took 85 ms when the A-line rate of the OCT system was set at 24 kHz. The calibrated depth resolution of the system was approximately 6 μm in the air and approximately 4.5 μm in the tissue (the refractive index of the whole mouse eye was approximately 1.475).

Data Analysis

The following refractive indices were used for the dimension calculation: 1.4015 for cornea, 1.3336 for aqueous, 1.3329 for vitreous, and 1.351 for retina.^{11,12} The refractive index of the lens was calculated by linear regression of the inhomogeneous lens index versus age.⁷ Data were analyzed by paired *t* test to determine the difference between two consecutive measurements. Statistical analysis was performed using SPSS software (version 10.0; SPSS Inc., Chicago, IL). Statistical significance was defined as a *P* value of less than .05.

RESULTS

Analysis for Normal Ocular Growth

Eyes of C57BL/6 mice were imaged when they were 28 and 82 days old. The figure shows the SD-OCT images and the normalized central A-line intensity signals of the same eye at 28 and 82 days of age, respectively.

The biometric measurements were obtained by measuring the distance between two locations in one OCT image. The OCT image was first displayed and enlarged in MATLAB software (MathWorks, Inc., Natick, MA) to visualize the pixels. The pixel coordinates in the depth and lateral directions can then be read using MATLAB tools. The axial length, corneal thickness, anterior chamber depth, lens thickness, vitreous chamber depth, and retinal thickness were all directly measured using an SD-OCT image acquired as one snapshot. The measured mean axial lengths of the mouse eye were $2,972.39 \pm 33.21 \mu\text{m}$ at 28 days and $3,161.80 \pm 20.06 \mu\text{m}$ at 82 days of age. The increase of axial length from 28 to 82 days of age was significant ($P < .001$). The detailed dimensions of the eye at 28 and 82 days of age are listed in Table 1. The corneal thickness, retinal thickness, and anterior chamber depth did not change significantly between 28 and 82 days of age ($P > .05$). However, lens thickness increased and vitreous chamber depth decreased significantly ($P < .001$ and $P = .001$, respectively).

Analysis of Form-Deprivation Myopia in Mice

Changes in the dimensions of the ocular components of form-deprived myopia in C57BL/6J mice were analyzed (Table 2). After 21 days of deprivation, high-resolution OCT images of both the right (deprived) and left (control) eyes were acquired. The interocular differences in axial length and vitreous chamber depth revealed statistically significant enlargement of the eye and the vitreous chamber in the deprived eyes ($P = .002$ and $.040$, respectively). In myopic eyes, there was a mean increase of $40.02 \mu\text{m}$ in axial length and $94.96 \mu\text{m}$ in vitreous chamber depth compared to the control eyes.

In contrast, no significant inter-ocular differences were observed in corneal thickness, anterior chamber depth, lens thickness, and retinal thickness ($P > .05$). It suggested that axial elongation of form-deprived myopia is mostly contributed by vitreous chamber depth increase.

DISCUSSION

This study provides a new method for measuring ocular dimensions of mice *in vivo*. In the mouse eye, changes in refraction of 1 diopter are equivalent to changes in axial length of only 5 μm according to the schematic eye model.⁷ High-frequency ultrasound was frequently used to measure ocular dimensions in tree shrew, chicken, and guinea pig models. However, high-resolution ultrasound (frequency up to 60 MHz) has a resolution limit of approximately 40 μm , equivalent to almost 10 diopters of refraction in a mouse eye. Video morphology and cryo-sections produce measurement errors of 80 and 140 μm , respectively.^{12,13} The highest resolution of micro MRI is approximately 24 μm and takes more than 30 minutes for one picture of an eyeball under anesthesia. Optical low coherence interferometer may have the same depth resolution as OCT, but the one-dimensional measurement makes inter-ocular comparison unreliable due to the unknown lateral position. Thus, the above methods are not a satisfactory choice for ocular development study in mice.

The major limitation in a previous study by Zhou et al. using TD-OCT to measure mouse eye dimension is its lower imaging speed, although it may have the same depth resolution as SD-OCT.⁹ In their study, to cope with the smaller imaging depth of the system, multiple cross-sectional images taken sequentially at different depth ranges were combined to take the measurements. Because the measurements were not from a single-shot image, their accuracy was limited.

In the current experiments, all of the ocular dimensions were acquired in one snapshot. The much faster image acquisition speed significantly reduced the influence of eye movement and decreased the required anesthesia time. Shortening the anesthesia duration can possibly reduce the risk of accidental death during anesthesia. It was reported that ketamine–xylazine anesthesia could cause hyperopic refractive shift in mice.¹⁴ Therefore, performing imaging on conscious mice may be preferred for study of myopia. The fast image acquisition speed makes SD-OCT suitable for measuring the ocular dimensions of conscious mice using specifically designed animal restrictions, which has been successfully tested in our laboratories (data not shown).

During normal development, the lens increased considerably in size from days 28 to 82 (from 1,622 to 1,870 μm), which resulted in a decline of the vitreous chamber depth (from 705 to 636 μm) even though the axial length increased. This developmental decrease in vitreous chamber depth due to prominent growth of the lens has also been reported in tree shrew eyes.³ This decrease in mice has been detected by using TD-OCT and frozen sections, but not with the optical low coherence interferometer.^{7–9} From 28 to 82 days, other ocular dimensions such as corneal thickness, anterior chamber depth, and retinal thickness did not change significantly. We can conclude that change of lens thickness is the primary cause of axial elongation in normal eye development.

We found that eyes with deprived myopia had longer axial length, which is caused primarily by increased vitreous chamber depth rather than lens thickness. A similar finding was reported by Tkatchenko et al. using micro MRI.¹⁰ It is widely accepted that the increase of vitreous chamber depth is the major cause of axial elongation in primate (including human)

myopia.^{15,16} The lens thickness tends to decrease in the deprived myopia eyes, although it does not reach a statistically significant level. This decrease is considered a compensation for axial elongation. Shih et al. reported in a large human population study that the lens in myopic eyes becomes much thinner to compensate for axial elongation.¹⁷

In the deprived myopia group, we found that the corneal thickness tends to increase and nearly reach a statistically significant level. However, there are no data in previous studies using micro MRI for comparison. Further investigation with a larger sample size is needed to make a conclusion.

We have demonstrated the capability of high-resolution SD-OCT for measuring ocular dimensions in mice. The success in biometric measurement in eye growth and the deprived myopia model of mice using a snapshot proved that SD-OCT is potentially a powerful tool that can be easily applied to research in eye development and myopia using small animal models. The imaging depth of SD-OCT can be further increased by eliminating the mirror image (complex conjugate in the Fourier transformation) using the various proven techniques. The imaging speed of SD-OCT can also be significantly increased by using a higher speed charge coupled device or complementary metal oxide semi-conductor camera. These techniques have been tested on human eyes in our laboratory and will be applied in animal experiments in the next step.

Acknowledgments

Supported in part by National Institutes of Health grant 7R21EB008800-02 to Dr. Jiao and R01 EY09828 to Dr. Fini.

REFERENCES

1. Waterston RH, Lindblad-Toh K, Birney E, et al. Initial sequencing and comparative analysis of the mouse genome. *Nature*. 2002;420:520–562. [PubMed: 12466850]
2. Bamber JC, Tristram M. Diagnostic ultrasound In: Webb S, ed. *The Physics of Medical Imaging*. Philadelphia: Adam Hilger; 1988:319–388.
3. Norton TT, McBrien NA. Normal development of refractive state and ocular component dimensions in the tree shrew (*Tupaia belangeri*). *Vision Res*. 1992;32:833–842. [PubMed: 1604852]
4. McBrien NA, Lawlor P, Gentle A. Scleral remodeling during the development of and recovery from axial myopia in the tree shrew. *Invest Ophthalmol Vis Sci* 2000;41:3713–3719. [PubMed: 11053267]
5. Rada JA, Wiechmann AF. Melatonin receptors in chick ocular tissues: implications for a role of melatonin in ocular growth regulation. *Invest Ophthalmol Vis Sci* 2006;47:25–33. [PubMed: 16384940]
6. Smith EL, 3rd, Huang J, Hung LF, Blasdel TL, Humbird TL, Bock-horst KH. Hemiretinal form deprivation: evidence for local control of eye growth and refractive development in infant monkeys. *Invest Ophthalmol Vis Sci* 2009;50:5057–5069. [PubMed: 19494197]
7. Schmucker C, Schaeffel F. A paraxial schematic eye model for the growing C57BL/6 mouse. *Vision Res* 2004;44:1857–1867. [PubMed: 15145680]
8. Schmucker C, Schaeffel F. In vivo biometry in the mouse eye with low coherence interferometry. *Vision Res* 2004;44:2445–2456. [PubMed: 15358080]
9. Zhou X, Xie J, Shen M, et al. Biometric measurement of the mouse eye using optical coherence tomography with focal plane advancement. *Vision Res* 2008;48:1137–1143. [PubMed: 18346775]

10. Tkatchenko TV, Shen Y, Tkatchenko AV. Mouse experimental myopia has features of primate myopia. *Invest Ophthalmol Vis Sci* 2010;51:1297–1303. [PubMed: 19875658]
11. Hughes A A schematic eye for the rat. *Vision Res* 1979;19:569–588. [PubMed: 483586]
12. Remtulla S, Hallett PE. A schematic eye for the mouse, and comparisons with the rat. *Vision Res* 1985;25:21–31. [PubMed: 3984214]
13. Tejedor J, de la Villa P. Refractive changes induced by form deprivation in the mouse eye. *Invest Ophthalmol Vis Sci* 2003;44:32–36. [PubMed: 12506052]
14. Tkatchenko TV, Tkatchenko AV. Ketamine-xylazine anesthesia causes hyperopic refractive shift in mice. *J Neurosci Methods* 2010;193(1):67–71. [PubMed: 20813132]
15. Wiesel TN, Raviola E. Myopia and eye enlargement after neonatal lid fusion in monkeys. *Nature* 1977;266:66–68. [PubMed: 402582]
16. Rosenfield M, Gilmartin B. *Myopia and Near Work*. Boston: Butterworth-Heinemann; 1998.
17. Shih YF, Chiang TH, Lin LL. Lens thickness changes among school-children in Taiwan. *Invest Ophthalmol Vis Sci* 2009;50:2637–2644. [PubMed: 19234352]

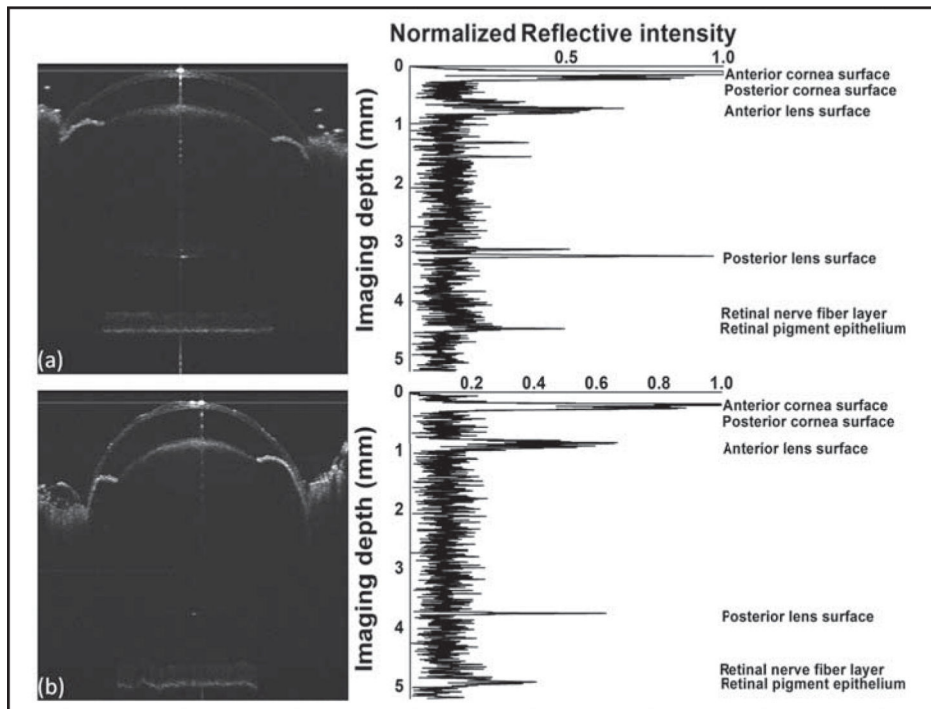


Figure.

Sample spectral-domain optical coherence tomography images and the corresponding intensity signal of the central A-line of a mouse eye at (A) 28 and (B) 82 days old. Axial length: from anterior corneal surface to the retinal pigment epithelium. Corneal thickness: from anterior corneal surface to posterior corneal surface. Anterior chamber depth: from posterior corneal surface to anterior lens surface. Lens thickness: from anterior lens surface to posterior lens surface. Vitreous chamber depth: from posterior lens surface to inner limiting membrane. Retinal thickness: from inner limiting membrane to retinal pigment epithelium

Mouse Ocular Dimensions Measured by Spectral-Domain Optical Coherence Tomography in Normal Ocular Growth

TABLE 1

Ocular Dimension	Mouse Eyeball		P
	28 Days	82 Days	
Axial length (µm)	2,972.39 ± 33.21	3,161.80 ± 20.06	< .001
Corneal thickness (µm)	98.74 ± 15.10	96.02 ± 9.49	.664
Anterior chamber depth (µm)	350.08 ± 12.10	360.55 ± 33.90	.342
Lens thickness (µm)	1,622.11 ± 10.72	1,870.71 ± 28.45	< .001
Vitreous chamber depth (µm)	705.53 ± 25.06	636.48 ± 42.31	.001
Retinal thickness (µm)	195.92 ± 8.91	198.04 ± 9.26	.08

Mouse Ocular Dimensions Measured by Spectral-Domain Optical Coherence Tomography in Form-Deprived Myopia and Control Eyes

TABLE 2

Ocular Dimension	Mouse Eyeball		P
	Myopia	Control	
Axial length (µm)	3,055.65 ± 39.63	3,015.63 ± 40.33	< .001
Corneal thickness (µm)	98.41 ± 8.11	84.62 ± 10.00	.054
Anterior chamber depth (µm)	330.35 ± 32.31	328.57 ± 16.33	.915
Lens thickness (µm)	1,712.92 ± 109.19	1,777.31 ± 65.97	.094
Vitreous chamber depth (µm)	718.67 ± 117.01	623.71 ± 59.21	.040
Retinal thickness (µm)	195.46 ± 16.30	201.10 ± 11.95	.466